

Journal *of* Medical Physics

Volume 47 | Issue 1 | January-March 2022

Full text at www.jmp.org.in



Association of Medical Physicists of India

An affiliate of Indian National Science Academy
and
International Organization for medical Physicists

www.ampi.org.in



Design and Evaluation of Structural Shielding of a Typical Radiotherapy Facility Using EGSnrc Monte Carlo Code

Zaccheaus Ayo Ibitoye, Margret Bose Adedokun¹, Temitope Aminat Orotoye², Godwin Bassey Udo

Department of Radiation Biology and Radiotherapy, College of Medicine, University of Lagos, Idi-Araba, ¹Department of Physics, University of Lagos, Akoka, ²Department of Radiotherapy, Mercelle Ruth Cancer Centre and Specialist Hospital, Ikoyi, Lagos, Nigeria

Abstract

Purpose: This study aimed to evaluate the shielding integrity of a typical radiotherapy facility using the Monte Carlo (MC) method. **Materials and Methods:** EGSnrc MC code was used to design a radiotherapy bunker with appropriate materials and thicknesses. A concrete density of 2.36 g/cm³ was used as a shielding material for primary and secondary barriers. The lead slab was used in the entrance door. The complex geometries of the bunker were modeled by using the egs++ application code embedded in the software. Phase-space generated from a linac machine built with BEAMnrc codes was used as a source of 18 MV X-ray beam set at 100 cm source–surface distance with a field size of 40 cm × 40 cm. Energy deposited in each geometrical region was evaluated and analyzed. **Results:** Energy deposited at the entrance door, supervised and controlled areas were found to be approximately 0%. No significant difference in the energy deposition on the geometries was observed when the gantry angles were set at either 90° or 270° ($P = 1$). **Conclusion:** The findings in this study revealed that the EGSnrc MC code can be used as a veritable tool in the design and evaluation of structural shielding efficiency in a radiotherapy facility.

Keywords: Concrete shielding, EGSnrc code, Monte Carlo, radiation protection

Received on: 04-06-2021

Review completed on: 28-09-2021

Accepted on: 30-09-2021

Published on: 31-03-2022

INTRODUCTION

Radiation exposure limits were introduced when the potential hazards of radiation were realized after the discovery of X-rays to protect radiation workers and the general public. Structural shielding design in medical radiotherapy installations is aimed to limit radiation exposures to members of the public and employees to an acceptable level.^[1,2] Shielding design is particularly concerned with the attenuation of the primary beam and secondary radiation in the form of head leakage, patient and wall scatter.^[3,4] To achieve the aforementioned objective, radiotherapy structural shielding facilities must be designed to minimize the need for relying on administrative controls and personal protective equipment for protection and safety during normal operation.^[1]

Optimum barrier thickness is an essential requirement for radiation safety around radiotherapy facilities as stated in the international basic safety standard (BSS) document.^[2] Furthermore, protective barriers are designed to ensure that the dose equivalent received by any individual does not exceed the applicable maximum permissible value. The areas surrounding

a radiotherapy treatment room are normally designated as either a controlled area or supervised area, depending on whether or not the exposure of persons in the area is under supervision. Shielding design for medical radiation therapy facilities is based on simple empirical equations reported in IAEA and NCRP documents.^[1,3]

Two principal radiation barriers in radiotherapy are routinely classified as primary and secondary barriers. Primary barriers are usually irradiated directly by the primary radiation beam from the target or source, while the secondary barrier receives radiation resulting from scattering of the primary beam by the patient and/or the surfaces of the treatment room in addition to the radiation transmitted through the accelerator head (i.e., head leakage radiation). Primary radiation is always limited in direction by the placement of the accelerator in the treatment

Address for correspondence: Dr. Zaccheaus Ayo Ibitoye, Department of Radiation Biology and Radiotherapy, College of Medicine, University of Lagos, Idi-Araba, Lagos, Nigeria. E-mail: azibitoye@cmlu.edu.ng

This is an open access journal, and articles are distributed under the terms of the Creative Commons Attribution-NonCommercial-ShareAlike 4.0 License, which allows others to remix, tweak, and build upon the work non-commercially, as long as appropriate credit is given and the new creations are licensed under the identical terms.

For reprints contact: WKHLRPMedknow_reprints@wolterskluwer.com

How to cite this article: Ibitoye ZA, Adedokun MB, Orotoye TA, Udo GB. Design and evaluation of structural shielding of a typical radiotherapy facility using egsnrc monte carlo code. *J Med Phys* 2022;47:27-33.

Access this article online

Quick Response Code:



Website:
www.jmp.org.in

DOI:
10.4103/jmp.jmp_76_21

room and the maximum beam size. Secondary radiation is, however, emitted in all directions and covers all the treatment room surfaces. The primary barrier is also expected to adequately attenuate dose equivalent beyond the barrier that may result in secondary products of the photon beam.^[1,4]

The usual materials for radiation shielding are normal or high-density concrete, steel, or lead. Concrete is mostly the first choice of shielding materials because it is cheap and readily available. Nevertheless, concrete densities are not as consistent as that of steel or lead, and they are therefore more difficult to monitor and control.

Shielding associated with radiotherapy equipment is very massive. Protecting adjacent occupancies typically requires several feet of reinforced concrete. In a typical treatment radiotherapy room, a maze (passageway) is introduced to reduce the radiation dose near the entrance and ensure that photon radiation can only exit the room after scattered radiation has been attenuated.^[4] Dose constraints in the controlled area and the supervised area must be part of planning when designing and constructing radiotherapy facilities.^[3] Radiation protection and safety on which the BSS is based must be considered when choosing appropriate dose constraints and optimization of protection and dose limitation.^[2]

Monte Carlo (MC) simulation is an accurate and detailed method for simulating complex source configurations and geometries in radiotherapy. Some of the available MC code systems for simulating electron and photon transport in a medium are EGSnrc, GEANT4, Penelope, Fluka, ETRAN, PHITS and MCNP. MC codes are also valuable in a critical method for accurate dose calculation, dosimetry evaluation, and design of treatment devices and components.^[5,6]

EGSnrc MC Software toolkit was employed in this study to perform simulation of ionizing radiation transport through the shielding structures.^[7] It is widely used to solve various problems in radiotherapy, especially to study radiation (photons, electrons and positrons) transport in materials. It is distributed with a wide range of applications that utilizes radiation transport physics to calculate specific quantities. Egs++ and tutor7pp application packages embedded in EGSnrc MC Software have some tools that aid in modeling complex geometries associated with the radiotherapy treatment room and assessing energy deposition into different shielding components, respectively.^[7,8]

The manual calculation has been the gold standard of determining acceptable barrier thickness according to recommendations and technical information provided in the NCRP 151 report for shielding design and evaluation in modern radiotherapy facilities. In this study, we conceptualized the application of MC code to design complex geometries of a radiotherapy facility that include high energy linac machine, shielding components, water phantom, and evaluation of radiation safety in the controlled and supervised areas with the aid of lithium fluoride (LiF). There is a paucity of information

on the use of MC code software to design radiotherapy bunkers and its application to evaluating radiation safety in the vicinity of a radiotherapy facility beyond manual calculation. Due to this, EGSnrc MC Code can be used as a quality assurance tool to ascertain radiation safety around radiotherapy facilities. In addition, it can be used during the preplanning arrangement to set up a radiotherapy department to reduce shielding materials cost and optimize available space.

Therefore, this study aimed to apply EGSnrc MC simulation methods to evaluate the structural shielding integrity of a radiotherapy facility before the installation of the linear accelerator (linac) machine since this is often impractical to perform experimentally after installation.

MATERIALS AND METHODS

Determination of barrier thickness

General assumptions

In this study, the shielding design goal *P* for the supervised area and controlled area was 0.02 mSv/week and 0.1 mSv/week, respectively. Occupancy factor, *T*, was 1. The use factor (*U*) for the primary barrier was set at 0.25. The workload (*W*) was 750 Gy/week (50 patients per working day, 3 Gy delivered dose at the isocenter per patient, and five working days per week) at 1 m source-axis distance (SAD). The dose rate at the isocenter (*DR₀*) was 12 Gy/min (720 Gy/h). The point of measurement at the protected location was 30.5 cm (1 ft) beyond the shielding walls. The dimensions used are shown in the layout depicted in Figure 1.

Primary barrier thickness

The thickness of the primary barrier *t_{pri}* was determined by using Equation 1;

$$t_{pri} = (TVL) \log_{10} \left(\frac{WUT}{P(d/d_0)^2} \right) \tag{1}$$

where *d* (= 7.75 m) is the distance from the isocenter to the locations *C₁* and *C₃*, *d₀* (= 1 m) is the SAD, and *Tenth* value

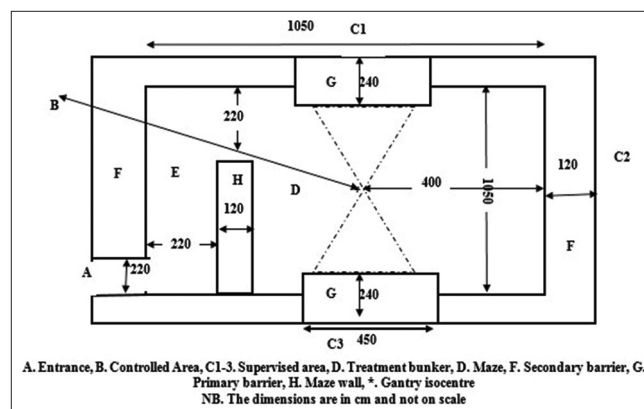


Figure 1: Schematic layout plan of a typical radiotherapy linac bunker facility. The machine gantry is perpendicular to the maze entry corridor. A lead-lined door of 10 cm thick was placed at entrance A and the height of the bunker was 900 cm

layer (TVL) (=445 mm) for the primary concrete used. From Equation (1), 2311.04 mm (231.1 cm) thick concrete thickness was obtained which is approximately equivalent to 240 cm barrier thickness used in this study to shield the public from radiation.

Dose rate at locations C1 and C3

Time average dose-equivalent rate per hour (TADR) (R_h) was calculated as 0.38 $\mu\text{Sv/h}$ using

$$R_h = IDR \frac{W_h U}{DR_0} \quad (2)$$

where instantaneous dose rate (IDR) was calculated as 0.76 $\mu\text{Sv/h}$ at location C1 and C3, W_n (=20 Gy/h) is the machine workload per hour, U (= 0.25) used factor for the primary barrier, and DR_0 (=12 Gy/min) dose output rate at the machine isocenter. The obtained value (0.38 $\mu\text{Sv/h}$) is much less than 20 $\mu\text{Sv/h}$ expected values in any hour requirement at these locations.

Secondary barrier thickness at location C2

Leakage radiation

The secondary barrier thickness (L_t) to shield the general public against leakage radiation at location C2 is determined from the equation below.

$$L_t = (TVL) \log_{10} \left(\frac{WT}{1000P(d_s / d_0)^2} \right) \quad (3)$$

where d_s (=5.5 m) is the distance from the isocenter to the location C2, d_0 is the distance between the source and the isocenter, and T (=1) occupancy factor, TVL (=330 mm) is the tenth-value layer required for leakage radiation. The minimum secondary barrier calculated to shield protect public against leakage radiation was 1020 mm (102 cm).

Scatter radiation

The secondary barrier thickness S_t required to shield against radiation scattered from the patient is determined from the equation below:

$$S_t = (TVL) \log_{10} \left(\frac{\alpha WT (F / 400)}{Pd_{sca}^2 d_{sec}^2} \right) \quad (4)$$

where d_{sca} (= 1 m) is the distance from the radiation source to the phantom, d_{sec} (5.5 m) is the distance from the phantom to point C1, α ($=3.75 \times 10^{-4}$) is the maximum scatter fractions of dose at 90° for a 400 cm², F (40 cm × 40 cm) is the field area incident on the phantom, and TVL (=174 mm of concrete) for patient scatter radiation at 90° scattered. With Equation (4) the minimum calculated barrier thickness was 569 mm. The thickness of the barrier (120 cm) used in this study was sufficient to shield the general public from leakage radiation and scattered radiation collectively.

Dose rate at location C2

The total instantaneous dose rate (IDR) for the leakage dose rate (= 0.38 $\mu\text{Sv/h}$) and scattered dose rate (= 0.192 $\mu\text{Sv/h}$) was calculated to be 0.572 $\mu\text{Sv/h}$ at location C. Therefore,

time average dose-equivalent rate per hour (TADR) (R_h) was obtained as 1.07 $\mu\text{Sv/h}$ (equation 2) which was much less than 20 $\mu\text{Sv/h}$ expected values in any hour requirement at location C.

Secondary barrier controlled area location B

Leakage radiation

The shielding required for protection against leakage radiation is determined from Equation (3). where P (=0.1 mSv/week) is the designed goal for the controlled area, d_s (=9.6 m) is the distance from the isocenter to location B, and TVL (=330 mm) for leakage radiation. A minimum thickness of 630 mm was required to shield the radiation workers at location B from leakage radiation in the controlled area.

Scatter radiation

The barrier transmission required to shield against radiation scattered by the patient is determined from Equation (4). d_{sca} (= 1 m) is the distance from the radiation source to the phantom, d_{sec} (9.6 m) is the distance from the phantom to point C1, α (= 0.00253) is the maximum scatter fractions of dose at 30° and 1 m, for a 400 cm², F (40 cm × 40 cm) is the field area incident on the phantom, and TVL (= 211 mm of concrete) for patient scatter radiation at 30° scattered. The calculated barrier thickness was 562 mm needed to shield against scattered radiation. A secondary barrier of 120 cm (1200 mm) as indicated in Figure 1 is sufficient to shield against leakage radiation and scattered radiation emanating from the phantom.

Dose rate at location B

The total instantaneous dose rate (IDR) for the leakage dose rate (= 0.98 $\mu\text{Sv/h}$) and scattered dose rate (1.84 $\mu\text{Sv/h}$) was calculated to be 1.84 $\mu\text{Sv/h}$. Therefore, the time average dose-equivalent rate per hour (TADR) (R_h) was obtained as 0.05 $\mu\text{Sv/h}$ (equation 2) which was much less than 20 $\mu\text{Sv/h}$ expected values in any hour requirement at location B.

Simulation and modeling

Two similar radiotherapy bunkers with dimensions shown in Figure 1 were modeled in this study. The first bunker consists of a typical bunker with all component media made of air (pre-shielding), while the second bunker has all its components consisting of appropriate materials such as concrete, lead, air, and detectors (LiF). EGS++ application code in the EGSnrc MC was used to model all these components. The modeled components were a secondary barrier, primary barrier, treatment room, maze, maze barrier, entrance door, leaded door, bunker vicinity, and thermoluminescent materials. The primary, secondary, and maze shield was made of concrete of density 2.35 g/cm³. The treatment room, maze, entrance and the vicinity of the bunker were made of air of density 0.00120479 g/cm³. The door was made of lead of density 11.36 g/cm³, while thermoluminescent material was made of lithium fluoride of density 2.635 g/cm³. Detectors 1–4 were placed at different locations inside the bunker, while detectors 5–8 were positioned in designated controlled and supervised

areas to evaluate radiation equivalent doses within and outside the treatment room.

Photon source

A linac with a photon beam energy of 18 MV acts as the source of radiation. This was modeled using the BEAMnrc code based on the EGSnrc MC technique (Kawrakow *et al.*, 2006). The linac head consists of the target, primary collimator, flattening filter, monitor chamber, mirror, secondary jaws, and exit window components.

In the present study, constant values of the global electron cutoff energy ($AE = ECUT = 0.7$ MeV) and the global photon cutoff energy ($AP = PCUT = 0.01$ MeV) were used for all component modules in the BEAMnrc simulations. The output of the linac machine was converted to a phase space (PhSp) file which contains data relating to particle position, direction, and charge. BEAMdp was used to evaluate the X-Y scatter plot from the phase-space file. The percentage depth dose at 100 cm source–surface distance (SSD) and 40 cm \times 40 cm field size was determined using DOSXYZnrc source code in a voxel water phantom geometry with dimensions of 60 cm \times 60 cm \times 80 cm to provide full scatter conditions. The phase-space file contains 21,854,648 particles (14,959,172 photons, 6,417,920 electrons, and 477,556 positrons) at a scoring plane of 100 cm from the target. The source was placed at an isocenter position inside the treatment room. The number of histories used was 21,854,648 particles and recycled 10 times to reduce statistical uncertainties.

Input definitions

The input definitions such as the geometry definitions, media definitions, particle source definitions, ausgabe definitions, and run control definitions were combined into an egs input file to execute the program. The file with the egsinp extension was placed in the tutor7pp code to determine the fraction of dose, energy, and particle deposited in each region of the simulated geometry framework. Simulations with and without water phantoms were also performed to evaluate the structural shielding integrity of the secondary barrier and primary barrier, respectively. The field size of 40 cm \times 40 cm placed at isocenter at 100 cm from the photon source was used. For a model with a water phantom, the same field size was used at an SSD of 100 cm. The machine gantry was rotated at angles 90° and 270° to face the primary barriers. We also assumed that the upper and the lower parts of the treatment room were not occupied. The output of the simulation was done by using Ausgabe input definitions. Electrons, positrons, and photons generated in each geometrical definition were tracked using the egs track scoring library. Energy deposited and dose were scored using the egs dose scoring library in all the defined regions. All other transport parameters and options were left at their default settings.

RESULTS

This section presents the results obtained in this study. Figure 2 shows a bunker with structural shielding components made of air (preshielding). Photon, electron, and positron

fluences generated are forward peaked. Energy deposited in the treatment room (bunker), vicinity of the bunker, and the primary wall that the beam was directed are 38.2%, 38.1%, and 20.9%, respectively, as shown in Figure 3. Bunker structural shielding components such as concrete, air, and lead and radiation particle fluence are shown in Figure 4. This figure shows that concrete as a shielding material for primary, secondary, and maze walls attenuates and constrains radiation particles without any form of radiation leakage. About 97% of the energy was deposited on the primary walls irrespective of the gantry directions, as shown in Figure 5.

Figure 6 shows the bunkers with water phantom to verify the integrity of the secondary walls. The figure shows that no leakage radiation was observed as a result of scattered radiations emanating from the exposed water phantom. About 70% of energy was deposited in the water phantom while primary walls received lesser energy deposition (24%), as shown in Figure 7. Scattered radiation generated from the water phantom increases the energy deposited in the secondary walls from 1.1% [Figure 5] to 4.2% [Figure 7].

Figure 8 shows the tracked particles generated during the simulation using a bunker with all its components made of air, a bunker with water phantom, and a bunker without water phantom. According to the figure, more photon particles were produced when the water phantom was placed at isocentre of the treatment room than when the water phantom was absent. In addition, more electron fluences were produced in the absence of the water phantom, this is because photoelectric and Compton effects dominate the interaction of photons with the air in the treatment room. Figure 9 shows instantaneous dose measured at different locations within and outside the bunker room. Instantaneous dose measured within the bunker using detectors 1–4 is greater than the dose recorded outside the bunker except for detector 3 which is at the maze area. Maze wall attenuates scattered radiation reaching detector

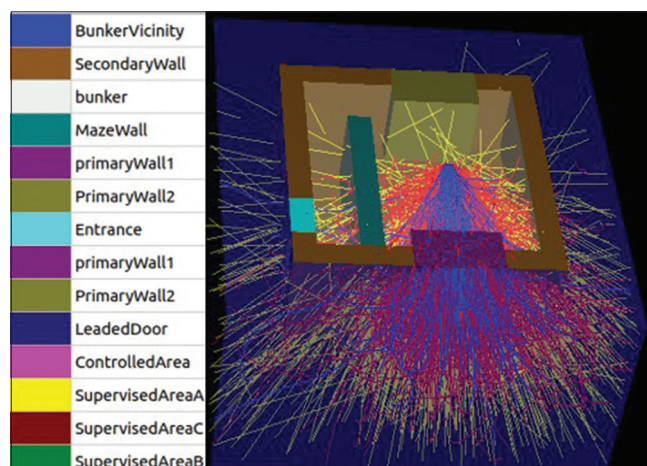


Figure 2: Particle fluence distribution in a bunker and its vicinity. Material components are made of air properties to assume a LINAC installation without any concrete barrier. Yellow, red, and blue radiation tracks represent photon, electron, and positron fluences, respectively

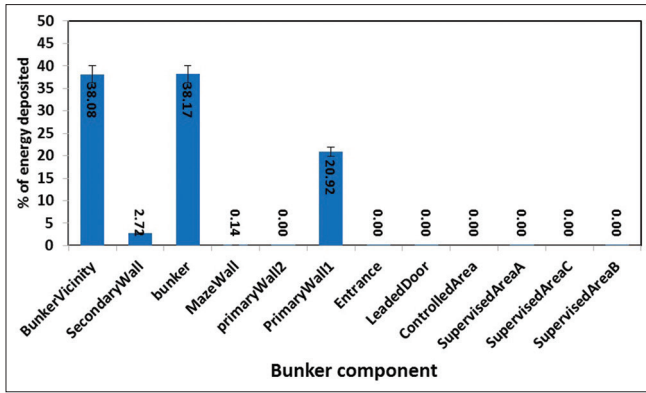


Figure 3: Percentage of energy deposited versus bunker components in a virtual bunker. Energy is more deposited in the bunker and the bunker vicinity than any other components. The linac was directed to primary wall1 which had 30.92% of the energy deposited. Other structural shielding components' percentage deposition values are shown in the figure

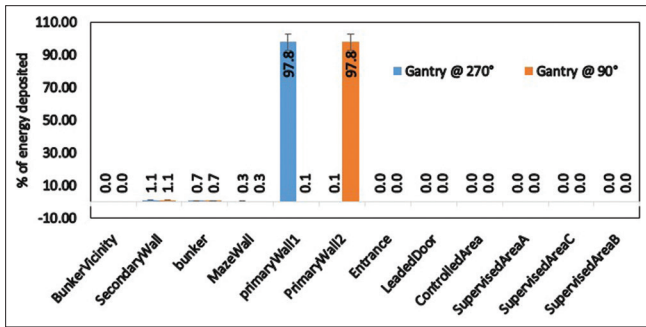


Figure 5: Percentage of energy deposited versus bunker components. The radiation primary beam faced the primary walls directly without a water phantom. About 97% of the energy was deposited on the primary walls irrespective of the gantry direction ($P = 1$). No energy was deposited around the bunker vicinities, maze entrance, leaded door, controlled area, and supervised areas A, B, and C

3 significantly. The value of doses recorded depends on the location of the detectors and the presence or absence of phantom during the irradiation.

DISCUSSION

In this study, we have designed a typical radiotherapy facility using EGSnrc MC software with a linac machine generating 18 MV beams installed at the isocenter. The design of the bunker was done with egs++ application, while energy deposited in each geometrical region was determined using tutor7pp user code. The dose rate at supervised areas and controlled areas [Figure 1] was far below 20 μSv in any hour requirement expected dose limit in the public area using calculation method (Equation 2).^[9] Particle fluence and percentage of energy deposited at every region were evaluated with the number of particles generated during the interactions of the photon with different media. The dose rate obtained using the MC method at different locations outside the bunker is far below 20 μSv which is in agreement with the empirical method [Figure 9].

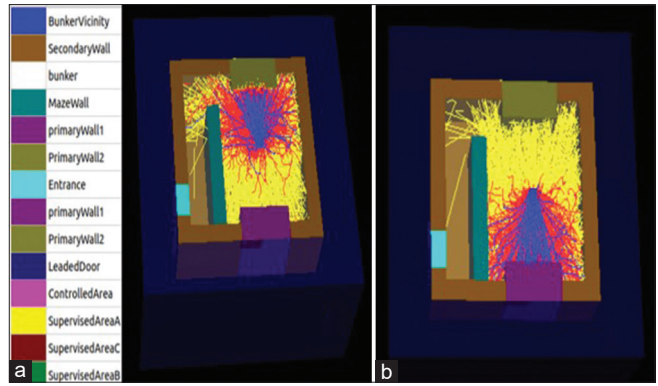


Figure 4: Bunker components and the radiation fluence in a bunker without a water phantom. Gantry was rotated at angles 90° (a) and 270° (b) using source-surface-distance 100 cm and field size 40 cm by 40 cm. The figure shows that radiation particle fluence was constrained by primary and secondary barriers. The maze wall prevents primary and scattered radiation from directly hitting the entrance, leaded door, and the wall on the secondary wall adjacent to it. The number of particle fluences in the maze depends on the gantry direction, as shown in the figure. No leakage radiation particle was observed

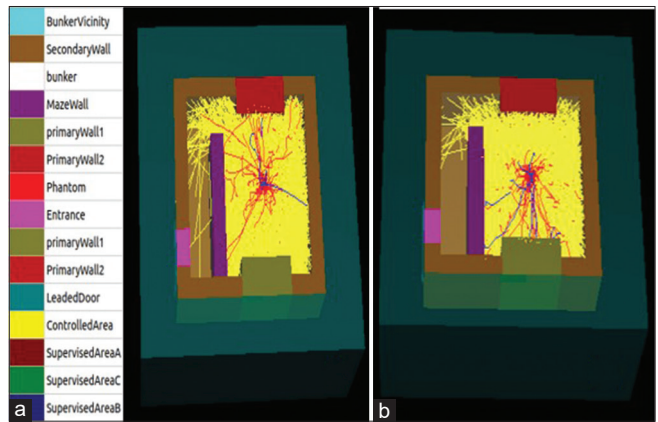


Figure 6: Bunker components and the radiation fluence with water phantom. Gantry rotated at angle 90° (a) and 270° (b) using 60 cm by 60 cm by 60 cm water phantom at source-surface distance 100 cm from the radiation source and 40 cm by 40 cm field size. In the figures, particle tracks were effectively constrained by primary and secondary barriers. The maze wall prevents direct hit of the entrance, leaded door, and the wall on the secondary wall adjacent to it by scattered and primary radiations (just as in the case without water phantom). The number of particle fluences in the maze depends also on the gantry directions. Scattering radiations from the irradiation of the water phantom dominate the fluence particles. No leakage radiation particle was observed in the bunker vicinity

According to this study, photon, electron, and positron fluences can be tracked in bunker components, as depicted in Figures 2, 4, and 6. The percentage of energy deposition in each component was determined and presented in Figures 3, 5, and 7. A bunker without concrete barriers (preshielding) can result in the deposition of about 38.1% of the radiation energy into the environment [Figure 3]. The presence of concrete as a shielding material reduces energy deposited in the bunker vicinity from 38.1% to 0.0% [Figures 6 and 8]. The percentage of energy deposited in the controlled and

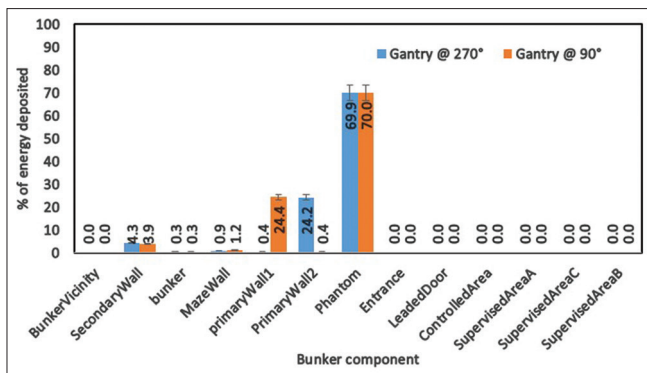


Figure 7: Percentage of energy deposited versus bunker with water phantom. The source to the water phantom surface distance was 100 cm. Energy deposited on the water phantom was about 70%, while that deposited on the primary wall was reduced to about 4% irrespective of the gantry rotation ($P = 1$). Energy deposited on the secondary wall was increased to about 4%. No energy was deposited around the bunker vicinities, maze entrance, leaded door, controlled area, and supervised areas A, B, and C

supervised areas was found to be approximately 0% as a result of the shielding materials [Figures 6 and 8]. Electron particles from photoelectric effects, Compton effects, and pair/triplet production accounted for the high number of particle fluence tracked during the simulation [Figure 7]. Maze in the bunker significantly helps to reduce scattered radiation reaching the interior part of the secondary barrier closed to the controlled room (detector 3), as shown in Figure 9.

The use of adequate shielding materials in the construction of barrier walls in the radiotherapy facility will help to achieve the radiation safety goal expected by the regulatory bodies. Empirical methods of calculation of the thickness of primary and secondary barriers by taking the occupancy and use factors into consideration are well-documented in the National Council on Radiation Protection and Measurements, NCRP report 151, and other documents.^[4,10,11] These reports also present recommendations and technical information related to the design and installation of structural shielding for megavoltage X- and gamma-ray radiotherapy facilities and have been used extensively. Some commercially available software such as MicroShield is also available to ease out complexities involved in the structural shielding calculation. Based on our knowledge, none of these provides real-time particle fluence distributions, energy, and dose deposited in the structural shielding components during their applications.

In this study, we were able to evaluate structural shielding integrity in a typical radiotherapy facility by using MC software. Radiation leakage, radiation fluence distribution, and energy deposition in each of the components within and around the radiotherapy facility were evaluated. Our findings in this study show that EGSnrc MC software could be applied as a veritable tool to assess the integrity of structural shielding

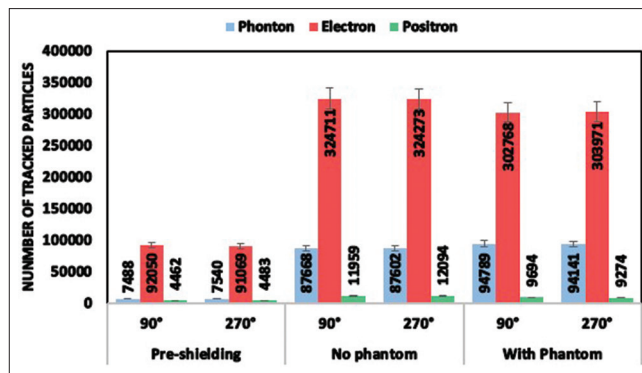


Figure 8: Number of tracked particles produced versus different modeling scenarios. The average photon particles generated with the water phantom in the bunker was 8.2% more than without phantom while electron particle fluences without water phantom were 6.7% greater than the bunker with water phantom set up. Since 18 MV beam energy (which is above the threshold energy of pair and triplet productions) was used positron particles were generated and tracked. On average, 19.4% of positron particles were produced more in a bunker without a water phantom than in a bunker with a water phantom

materials in radiotherapy facilities. It can also be used to estimate and predict radiation particle fluence distributions in a bunker in terms of structural shielding components before the installation of the radiotherapy equipment. The use of the MC method described in this study can be an additional method of evaluating the level of radiation protection around radiotherapy facilities during radiotherapy procedures. Neutron fluence produced as a result of using high-energy photons could not be evaluated since the EGSnrc MC code is yet to be equipped with a package to study this.

Based on the previous studies, MC simulation has been considered to be the most accurate tool to describe the underlying physical interactions between radiation and matter. EGSnrc MC Software has been successfully used in various dosimetry principles,^[12,13] HVL evaluation of orthovoltage machine,^[14] simulation of radiotherapy treatment units,^[15-18] beam quality correction factor,^[19] and so forth. Furthermore, previous studies have shown that MC can be used in the evaluation of X-rays transmission through some shielding materials,^[11] evaluation of the attenuation coefficient of personal radiation shielding protective clothing,^[20] determination of shielding properties of concrete,^[21] shielding analysis,^[22] and the simulation of X-ray room shielding in diagnostic radiology.^[23] However, there is a paucity of information on the application of the EGSnrc MC code in the design of radiotherapy bunker and evaluation of radiation protection around the facility.

The findings in this study show that the EGSnrc MC code can be extended to the principle of radiation protection to evaluate dose and energy deposition in the primary barrier, secondary barrier, maze, entrance door, controlled area, and supervised area effectively before and after installation of the radiotherapy machines.

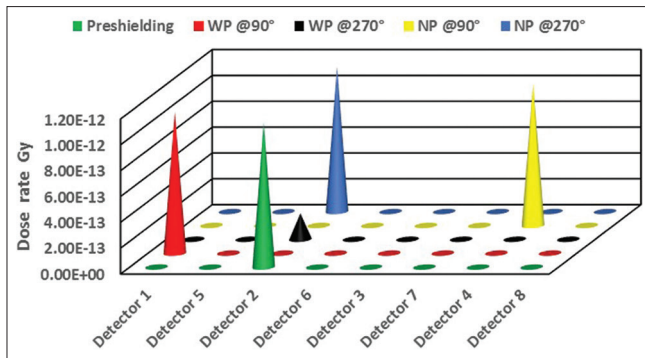


Figure 9: Instantaneous dose rate distribution within and outside the bunker using TLDs as detectors. Detectors 1–4 recorded higher doses because they were placed strategically at different locations inside the bunker. No significant dose was recorded by detector 3 because the maze wall attenuates scattered radiation considerably. Doses recorded by detectors 5–7 placed controlled area and supervised areas were significantly low. WP: Water phantom, NP: No phantom

CONCLUSION

The findings obtained in this study show that EGSnrc software is a veritable tool that can be applied to evaluate structural shielding integrity in radiotherapy facilities. It has the potential to be used to design structural complexities of radiotherapy bunker as well as provide a broad knowledge of radiation particle fluence distributions during the radiotherapy procedures. In addition, it can be used to determine appropriate shielding requirements whenever an old bunker built purposely to accommodate lower energy is modified for high-energy linac facilities. Finally, MC methods can also be used to evaluate radiation leakage and instantaneous dose rate in the supervised and controlled areas as well as scatter radiation at the entrance door of the radiotherapy facilities before and after the installation of the radiotherapy machine.

Financial support and sponsorship

Nil.

Conflicts of interest

There are no conflicts of interest.

REFERENCES

1. IAEA (International Atomic Energy Agency). Radiotherapy Facilities: Master Planning and Concept Design Considerations IAEA Human Health Reports No. 10. Vienna: IAEA; 2014.
2. European Commission, Food And Agriculture Organization of The United Nations, International Atomic Energy Agency, International Labour Organization, OECD Nuclear Energy Agency, Pan American Health Organization, United Nations Environment Programme and World Health Organization. Radiation Protection and Safety of Radiation Sources: International Basic Safety Standards, IAEA Safety Standards Series No. GSR Part 3. Vienna: IAEA; 2014.
3. IAEA (International Atomic Energy Agency). Radiation Protection in the Design of Radiotherapy Facilities. IAEA Safety Reports Series No. 47. Vienna: IAEA (International Atomic Energy Agency); 2006.

4. NCRP (National Council on Radiation Protection). Structural Shielding Design and Evaluation for Megavoltage X- and Gamma-Ray Radiotherapy Facilities, NCRP Report 151. Bethesda: NCRP (National Council on Radiation Protection); 2005.
5. Bielajew A. The monte carlo simulation of radiation transport. In: Mayles P, Nahum A, Rosenwald JC, editors. Handbook of Radiotherapy Physics: Theory and Practice. CRC Press, Boca Raton, FL: Taylor & Francis Group; 2007. p. 75-87.
6. Kawrakow I, Mainegra-Hing E, Rogers DW, Tessier F, Walters BR. The EGSnrc code system: Monte carlo simulation of electron and photon transport. In: Technical Report PIRS-701. Ottawa: National Research Council of Canada; 2017.
7. Kawrakow I, Mainegra-Hing E, Tessier F, Townson R, Walters B. The EGSnrc C++ class library. In: Technical Report PIRS-898, Ottawa. Ottawa: National Research Council of Canada; 2019.
8. Lopez PO, Rajan G, Podgorsak EB. Radiation protection and safety in radiotherapy. In: Podgorsak EB, editor. Radiation Oncology Physics: A Handbook for Teachers and Students. Vienna: IAEA; 2005. p. 604-5.
9. Nuclear Regulatory Commission. Standards of Protection against Radiation, 10CFR20, US Office of the Federal Register. Washington, DC: Nuclear Regulatory Commission; 1991.
10. Morrow Mc A. Radiation shielding and bunker design. Biomed J Sci Tech Res 2019;18:13320-30.
11. Al-Ghorabie F, Al-Lyhiani S, Natto S. EGSnrc computer modelling of megavoltage x-rays transmission through some shielding materials used in radiotherapy. J Radiother Pract 2010;9:223-36.
12. Painuly NK, Singh N, Verma TR, Chairmadurai A, Chaudhari LN, Saily A, *et al.* Evaluation of dose perturbation at the interface of two different density medium using GAFCHROMIC film EBT2 and Monte Carlo code EGSnrc for Co-60 beam. J Can Res Ther 2015;11:775-9.
13. Al Kanti H, El Hajjaji O, El Bardouni T, Boukhal H, Mohammed M. Conversion coefficients calculation of mono-energetic photons from air-kerma using Monte Carlo and analytical methods. J King Saud Univ Sci 2020;32:288-93.
14. Monfared AS, Pourfallah TA, Babapour H, Shirazi AV. HVL evaluation of orthovoltage X-ray machine using EGSnrc code of simulation. Int J Radiat Res 2014;12:325-30.
15. Rogers DW, Faddegon BA, Ding GX, Ma CM, We J, Mackie TR. BEAM: A Monte Carlo code to simulate radiotherapy treatment units. Med Phys 1995;22:503-24.
16. Sung W, Park JI, Kim JI, Carlson J, Ye SJ, Park JM. Monte Carlo simulation for scanning technique with scattering foil free electron beam: A proof of concept study. PLoS One 2017;12:e0177380.
17. Jabbaria N, Barati AH, Rahmatnezhad L. Multiple-source models for electron beams of a medical linear accelerator using BEAMDP computer code. Rep Pract Oncol Radiother 2012;17:211-9.
18. Gholamourkashi S, Cygler JE, Belec J, Vujicic M, Heath E. Monte Carlo and analytic modelling of an Elekta infinity linac with Agility: Investigating the significance of accurate model parameters for small radiation fields. J Appl Clin Phys 2019;20:55-67.
19. Choi SH, Kim CH, Huh HD, Kim KB, Kim SH. Determination of the beam quality correction factor kQ₀ for the micro Lion chamber in a clinical photon beam. J Korean Phys Soc 2013;62:152-8.
20. Kozlovska M, Solc J, Otahal P. Measuring and monte carlo modelling of X-ray and gamma-ray attenuation in personal radiation shielding protective clothing. Comput Math Methods Med 2019;2019:1641895.
21. Khaldari R, Mesbahi A, Kara U. Monte Carlo calculation of shielding properties of newly developed heavy concretes for megavoltage photon beam spectra used in radiation therapy. Iran J Med Phys 2016;13:250-60.
22. Ródenas J, Martinavarró A, León A, Verdú G. Application of the Monte Carlo Method to shielding analysis in medical linear accelerators. J Nucl Sci Technol 2000;37:441-5.
23. Abdul-Aziz MZ, Yani S, Haryanto F, Kamarullah Ya Ali N, Tajudin SM, Iwase H, *et al.* Monte Carlo simulation of X-ray room shielding in diagnostic radiology using PHITS code. J Radiat Res Appl Sci 2020;13:704-13.